NaBF as a hygrothermal durability enhancer for glass fibre reinforced polypropylene composites

R.-C. Zhuang, J.-W. Liu, R. Plonka, Y.-X. Huang, E. Mäder

$NaBF_4$ as a hygrothermal durability enhancer for glass fibre reinforced polypropylene composites

R.-C. Zhuang, J.-W. Liu, R. Plonka, Y.-X. Huang, E. Mäder

PII: S0266-3538(11)00207-7
DOI: 10.1016/j.compscitech.2011.06.002
Reference: CSTE 5001

To appear in: *Composites Science and Technology*

Received Date: 18 January 2011
Revised Date: 3 June 2011
Accepted Date: 10 June 2011

Please cite this article as: Zhuang, R.-C., Liu, J.-W., Plonka, R., Huang, Y.-X., Mäder, E., $NaBF_4$ as a hygrothermal durability enhancer for glass fibre reinforced polypropylene composites, *Composites Science and Technology* (2011), doi: 10.1016/j.compscitech.2011.06.002

$NaBF_4$ as a hygrothermal durability enhancer for glass fibre reinforced polypropylene composites

R.-C. Zhuang[a], J.-W. Liu[a], R. Plonka[a], Y.-X. Huang[b], E. Mäder[a*]

[a] Leibniz-Institut für Polymerforschung Dresden e.V., Hohe str. 6, 01069 Dresden, Germany

[b] Department of Materials Science and Engineering, College of Materials, Xiamen University, Xiamen, 361005, China

[*] Corresponding author. Tel.: +49 (0) 351 4658 305; fax: +49 (0) 351 4658 362. E-mail address: emaeder@ipfdd.de (E. Mäder)

Abstract

The long term performance of composite materials is highly desired for their expanding application range. Tuning the interphase properties has been proven to be a practical way to enhance the performance of composites. In this study, short glass fibre (GF) reinforced polypropylenes (PPs) with improved hygrothermal durability were obtained by incorporating $NaBF_4$ into the sizing and thus the interphases of GF/PP composites. Detailed investigations were performed on the surface properties of sized GFs and the mechanical properties of virgin and aged composites. It was found that the retention in both ultimate tensile strength and Charpy impact toughness of aged composites monotonically increased with increasing $NaBF_4$ content. The improvement in hygrothermal durability was related to the enhanced fibre/matrix adhesion strength induced by the presence of $NaBF_4$ as indentified by fracture surface analysis using field-emission scanning electron microscopy and single fibre pull-out test.

Key words: A. Glass fibres, A. Polymer-matrix composites (PMCs), B. Durability, B. Interphase, B. Surface treatments

1. Introduction

Owing to the combination of great static/dynamic mechanical properties, recyclable feature, low cost, and tailor-able polymer structure, PP is one of the most intense used semi-crystalline polymers, gaining a wide variety of applications [1, 2]. Furthermore, the incorporation of high stiffness and high strength fibres into PP realized fibre reinforced PP composites with significantly improved stiffness and strength, which greatly expands the use range of PP to more broader application fields, such as structural or semi-structural materials in automotive, offshore, and marine structures [3, 4]. This, in turn, demands fibre reinforced PP composites with improved long term performance in different environments, such as moisture, temperature, radiation.

Influenced by moisture and elevated temperature, i.e. hygrothermal aging, fibre reinforced polymers usually suffer significant performance degradation [5, 6]. Several mechanisms accounting for the performance reduction have been proposed involving the following interactions between water and the constitutes of composites [7, 8]. It has been observed that water molecules could 1) diffuse to matrix and reinforcing fibre leading to the degradation of matrix and fibre, 2) penetrate to the interphase between matrix and fibre resulting in de-bonding, and 3) transport through microcracks or other forms of microdamages, such as pores or small channels, giving rise to the build up of stress. Experiments also revealed that the uptake of moisture mostly follows Fick's law of diffusion with different diffusion coefficients, which increase with increasing temperature but decrease with increasing water salinity [9]. In addition, it was estimated that water penetrating through interphases was more than 450 times faster than through matrix [10]. Hence, surface modification of reinforcing fibres with sizings/coatings and incorporation of matrix modifier are two common means used to improve the hygrothermal stability of fibre reinforced polymers by enhancing the interfacial adhesion strength or impenetrability [10-12]. Thus, the water penetration was limited and the deterioration on matrix, fibre and interphase was slowed down [10].

The interphase between reinforcement and matrix plays an important role in determining the mechanical properties of composites [13]. In GF/PP composites the interphase between GF and PP is formed by the interdiffusion of matrix PP and the sizing of GFs. This results in the interpenetrating networks (IPNs) of polysiloxane and PP, where siloxane groups and maleimide groups are created for polysiloxane/GF and polysiloxane/maleic anhydride grafted PP (MAH-*g*-PP, matrix modifier), respectively [14]. Consequently, stress can be efficiently transferred from matrix to load bearing reinforcing fibres leading to GF/PP composites with great performance. Besides these perfect covalent bondings, there are still some un-reacted silanol groups, polar groups of lubricants or surfactants [15] and other weak points in the interphase, which are liable to interact with [16] and accommodate water molecules, leading to the degradation of interphase properties, correspondingly, the mechanical properties of composites. When the non-hygroscopic features of GFs and PP are taken into consideration [17], it becomes obvious that proper interphase design holds great promise to improve the hygrothermal durability of composites [3]. However, as yet reports addressing the further improvement of the hygrothermal durability of GF (the most widely used fibre reinforcement globally) reinforced PP composites are rather limited.

Tetrafluoroborate ion (BF_4^-) is being used as the counter ion of templating agents for the preparation of mesoporous silica with higher thermal and hydrothermal stabilities in comparison with fluoride ion, which is mainly attributed to the less-hydrophilic BF_4^- promoting the hydrolytic condensation of alkoxysilanes [18, 19]. Meanwhile, it has been reported that O-B-F was formed in hydrothermally synthesized borophosphates [20] or the hydrolysis of BF_4^- ion [21]. It suggests that F could be chemically coupled to silica. Taking into consideration the chemical similarity for silica, GF and the polysiloxane in the interphase of GF/PP, the introduction of tetrafluoroborate ions into the interphase might lead to interphases with higher hydrophobic character and higher hygrothermal stability, correspondingly, GF/PP with higher hygrothermal durability.

In this work, we present the results on the concept: Enhancing the hygrothermal durability of composites by "hydrophobizing" the interphase. The potential of $NaBF_4$ was assessed as "interphase hydrophobizer". The work focuses on the influence of $NaBF_4$ content on the fibre properties and hygrothermal stability of short GF/PP composites with both PP homopolymer and PP-polyethylene copolymer as matrices. Field-emission scanning electron microscopy (FE-SEM) was used to investigate the fracture surfaces of tensile test specimens. Single fibre pull-out test (SFPO) was used as a complemental method. The correlation between fibre/matrix adhesion strength and hygrothermal durability is discussed.

2. Experimental Details

2.1 Materials and sample preparation

E-GFs sized by 3-aminopropyltriethoxysilane (AMEO, Evonik Degussa GmbH, Rheinfelden, Germany) in conjunction with a PP film former (Permanol 602，Clariant, Switzerland) in presence of or free of additive ($NaBF_4$, Sigma-Aldrich, Germany) were spun at the Leibniz Institute of Polymer Research Dresden using continuous spinning devices comparable to industrials ones. The average diameter of used sized GFs was 17 μm. The content of $NaBF_4$ in sizings was 0.0, 0.08, 0.16, and 0.32 wt%, respectively. The addition of $NaBF_4$ did not affect the pH value of the sizings. These sized GFs are referred to as GF-00, GF-08, GF-16, and GF-32, respectively. An isotactic PP homopolymer (Hostalen PP W2080, LyondellBasell Industries) and a PP copolymer (Moplen EP240T, LyondellBasell Industries) compounded with 2 wt% PP-*g*-MAH (Exxelor PO1020) were used as matrices and referred to as PPH (crystallization enthalpy ΔH_c = 110.9 J/g) and PPC (ΔH_c = 81.4 J/g), respectively. GF/PPs with 30 wt% GF (13.2 vol%) were compounded using a co-rotating twin-screw extruder ZSK 30 (Werner & Pfleiderer, Stuttgart, Germany). Consequently, eight composites were made, they are designated by (matrix type)-($NaBF_4$ content). For example, PPH-32 is the PPH based composite reinforced with GF-32. The dog-bone shaped specimens (160×10×4 mm, according to DIN 53455, specimen No. 3, ISO 527.2) and plates (80×4×2 mm) were made on

the injection moulding machine Ergotech 100 (Demag Ergotech Wiehe GmbH) for tensile strength test and Charpy impact test, respectively.

2.2 Characterizations

The loss on ignition (LOI) of sized GFs was determined according to ASTM D4963-04 by means of high temperature pyrolysis at 625 ^{o}C. Fibre content of composites was also estimated gravimetrically by the resin burn-off method (ASTM D2584).

Tapping mode Atomic Force Microscope (AFM) investigations were carried out on a Dimension 3100 (Digital Instruments, Santa Barbara) at room temperature. The values of root-mean-square roughness (R_q) and maximum height roughness (R_{max}) were calculated after 2nd flatten over the whole captured area (3×3 μm^2).

Dynamic advancing contact angle (θ_a) and receding contact angle (θ_r) measurements on single GFs were performed on a tensiometer K14 (Krüss GmbH, Hamburg, Germany).

X-ray photoelectron spectroscopy (XPS) investigations were performed on a Kratos AXIS Ultra X-ray photoelectron spectrometer. Areas of approximate 300×700 μm^2 were analyzed with a monochromatic Al Kα X-ray source. The survey spectra were collected over a wide binding energy range (0-1300 eV) and were used to evaluate all of the elements present (except H and He) within the sample surface. The survey spectra were acquired at a pass energy of 160 eV and a step size of 1 eV. The high resolution spectra were obtained at a pass energy of 20 eV and dissected by means of the spectra deconvolution software. The parameters of the component peaks were their binding energy, height, full width at half maximum, and the Gaussian-Lorentzian ratio. The maximum information depth of 8 nm was probed with take-off angle 90 ^{o}.

The modulated DSC was carried out on a Q 2000 MDSC (TA Instruments, USA) at a temperature change rate of 10 K/min.

Hygrothermal aging was carried out in 95 ^{o}C de-ionized water for 10 days in an autoclave (CV-EL 18 L GS, CertoClav Sterilizer GbmH, Traun, Asutria). Hygrothermal aging

led to water uptake in the range of 0.23 to 0.32 wt%, which did not show clearly correlation with $NaBF_4$ content. The aged specimens were stored in air-conditioned room (50 % relative humidity, 23 ^oC) for 24 hours before mechanical property test.

Tensile tests were performed on a Zwick 1456 Universal Testing Machine (Zwick GmbH, Ulm, Germany) according to ISO 527-2/1A/5. The presented results are averaged values based on 10 specimens for each test series. Unnotched Charpy impact tests were carried out on a PSW 4J (Zorn GmbH, Stendal, Germany) in accordance with ISO 179/1eU. The presented results are averaged values based on 5 specimens for each test series.

The retention of composite tensile strength and Charpy impact toughness after hygrothermal aging is defined as:

$$\Delta\sigma = \sigma_{aged} / \sigma_{DAM} \times 100\% \quad (1)$$

and $\Delta a_{cU} = a_{cU_{aged}} / a_{cU_{DAM}} \times 100\%$, (2)

respectively, where σ_{aged} and σ_{DAM} are the ultimate tensile strength of aged and dry as molded (DAM) composites, respectively. $a_{cU\ aged}$ and $a_{cU\ DAM}$ are the Charpy impact toughness of aged and DAM composites, respectively. In order to further reveal the impact of $NaBF_4$ content, the relative change in mechanical properties of composites with $NaBF_4$ over composites without $NaBF_4$ is calculated using following equations:

$$\Delta\sigma_{DAM} = \left(\sigma_{DAM,NaBF_4\%} - \sigma_{DAM,0.0\%}\right) / \sigma_{DAM,0.0\%} \times 100\%, \quad (3)$$

$$\Delta\sigma_{aged} = \left(\sigma_{aged,NaBF_4\%} - \sigma_{aged,0.0\%}\right) / \sigma_{aged,0.0\%} \times 100\%, \quad (4)$$

$$\Delta a_{cU_{DAM}} = \left(a_{cU_{DAM,NaBF_4\%}} - a_{cU_{DAM,0.0\%}}\right) / a_{cU_{DAM,0.0\%}} \times 100\%, \quad (5)$$

and $\Delta a_{cU_{aged}} = \left(a_{cU_{aged,NaBF_4\%}} - a_{cU_{aged,0.0\%}}\right) / a_{cU_{aged,0.0\%}} \times 100\%$. (6)

Equations (3) and (4) give the relative tensile strength changes for DAM and aged composites, respectively. Equations (5) and (6) present the relative Charpy impact toughness changes for DAM and aged composites, respectively. The subscript $NaBF_4$% means the wt% of $NaBF_4$ in sizing multiplied by 100. The subscript 0.0% stands for composites without $NaBF_4$.

The fracture surface of tensile test specimens was investigated by using a FE-SEM (Ultra 55, Carl Zeiss SMT AG, Germany). The samples for SEM observation were coated by approximately 5 nm thick platinum layer.

SFPO on single fibre model composites was performed on home-made equipment to study the interfacial adhesion strength. The fibres were end-embedded around 800 μm deep into matrix at 200 ^{o}C or 250 ^{o}C for 210 s in Ar for PPH and PPC, respectively. The pull-out apparatus allowed investigators to obtain force–displacement curves of the single fibre composites under quasi-static conditions with a loading rate of 0.01 μm/s at ambient conditions. For the experimental data treatment, the latest approaches are used to determine interfacial adhesion strength, τ_d, frictional strength (also referred as interfacial stress in debonded regions), τ_f, and critical energy release rate, G_{ic} [22].

3. Results and discussion

3.1 Surface properties of sized GFs

Firstly, the influence of $NaBF_4$ content on the surface properties of differently sized GFs was studied by determining the LOI of sized GFs. Table 1 shows that the LOI of sized GFs with low $NaBF_4$ contents was similar to that of sized GFs without $NaBF_4$ while an increase of LOI value was obtained for GF-32. This suggests that the sizing containing 0.32 wt% $NaBF_4$ might have different physicochemical properties compared to reference sizing, in order to better understand the influence of $NaBF_4$ on the physicochemical properties of sizings, ongoing comprehensive work will be published elsewhere.

Tapping mode AFM was used to study the surface topography and surface roughness of differently sized GFs. The three-dimensional AFM height images (Fig. 1) clearly show that all sized GFs possess similar “island in sea” topography characterized by randomly distributed small aggregates of different sizes. It indicates that the addition of $NaBF_4$ to sizings hardly changed the surface topography of sized GFs, whatever how much $NaBF_4$ (within the range of this work) was incorporated. Correspondingly, the R_q and R_{max} of differently sized GFs

exhibited no difference and were in the range of 9.2−12.9 nm and 93.1−121.2 nm, respectively (Table 1). In addition, the R_{max} values are close to the mean particle size of PP film former [23], this suggests that the aggregates were mainly made of PP particles.

The influence of $NaBF_4$ content on the surface properties of sized GFs was further evaluated by determining the hydrophobicity of sized GFs using dynamical contact angle measurement. Table 1 summarizes θ_a and θ_r values. It was found that θ_a of differently sized GFs was quite close to each other and in the range of 83.0−84.7 °. On the other hand, θ_r of GF-32 was only 52.6 °, which was a little lower than that (60.9−62.6 °) of other three sized GFs. Taking into consideration the similar topography and surface roughness for all four sized GFs, the lower θ_r for GF-32 is most likely attributed to its higher sizing uptake, since it was noted previously that the GFs sized only with the same PP film former used here exihibited low θ_r of 41.6 ° [23]. This will be further described in next part.

The surface chemical composition of sized GFs was determined by XPS, the normalized average surface composition of C, N, F, Na, B and Si atoms in at% are tabulated in Table 1. Here, Ca atom is used as reference instead of Si atom because of the "island in sea" topography and low LOI of sized GFs [23, 24]. It is noted that the reference fibre GF-00 was free of F atom as expected; meanwhile the Na at% was relatively low and in the range of normal E-GF. The incorporation of $NaBF_4$ into sizing led to the introduction of F atom in sized GF surfaces (Fig. 2 and Table 1). The normalized F and Na at% increased monotonically with increasing $NaBF_4$ content while the normalized Si and O at% decreased gradually. These observations indicate that the $NaBF_4$ amount in the sized GF surface increased as the $NaBF_4$ content of sizings increased. Interestingly, it is noted that the normalized C at% showed firstly a small increase for GF-08 and GF-16, then a significant increment for GF-32. On the other hand, the normalized N at% exhibited a reverse tendency as C at%. It suggests that the addition of $NaBF_4$ in sizing resulted in sized GFs with higher PP film former content in the sizing/air

interface and higher protonation degree for amino groups, both of which increase with increasing $NaBF_4$ (detailed analysis refers to Appendix).

From above discussion, it is obvious that the incorporation of $NaBF_4$ into sizing did not alter the surface properties of sized GFs in terms of surface topography, surface roughness and surface hydrophobicity. On the other hand, the surface chemical composition of sized GFs varied with the variation in $NaBF_4$ content. The increase of $NaBF_4$ content in sizing led to not only the monotonic increase of $NaBF_4$ amount but also first slow then significant increase in PP film former content in the outermost surface of sized GFs.

3.2 Composite performance

Tensile and Charpy impact tests on DAM and aged composites were performed to evaluate the influence of $NaBF_4$ on the composite mechanical properties and hygrothermal durability. Fig. 3 shows the stress-strain curves for DAM and aged PPH-00, PPH-32, PPC-00, and PPC-32. It is noted that the application of $NaBF_4$ hardly influenced on the ultimate tensile strength, σ, of all DAM composites. On the other hand, DAM composites of PPH achieved higher σ but smaller elongation at break in comparison with those of PPC. This can be explained by the difference in the contribution of matrices based on following observations: 1) a brittle like fracture or very weak plastic deformation of PPH was observed for PPH based composites, 2) PPC based composites showed much pronounced plastic deformation of matrix due to the incorporated PE (cf. Fig. 6 and 7) [25]. Upon hygrothermal aging, all composites showed lower ductility, which was manifested by the reduction in the elongation at break. The aged PPH-00 fractured without yielding and exhibited a pronounced reduction in both σ and elongation at break, while aged PPC-00 broke right after yielding associated with a small reduction in σ. The reduction in both σ and elongation at break for aged PPH-00 after hygrothrmal aging is most likely related to the debonding between GF and PPH (cf. Fig. 6), which lessened the efficiency of stress transfer of the interphases. In the case of aged PPC-00, the nearly intact σ is similar to that of rubber toughened semi-crystalline polymers [26] and

most likely related to the embrittlement of PE regions, since less plastic yielding of matrix was observed on the fracture surfaces (Fig. 7). Interestingly, the incorporation of $NaBF_4$ could enhance the hygrothermal durability for both PPH and PPC composites, aged PPH composites with $NaBF_4$ achieve not only higher σ but also larger elongation at break, and improvement in elongation at break was observed for aged PPC composites. This is mostly due to the enhanced fibre/matrix adhesion strength (cf. Fig. 6 and 7). In addition, it was found PPH composites suffered greater yellowing while only slight yellowing was observed for PPC composites (cf. inset of Fig. 3). It is consistent with the better hygrothermal durability of PPC composites, which have less tertiary H that is liable to oxidation leading to molar mass reduce and discoloration [27].

The detailed influence of $NaBF_4$ on the composite performance is discussed in following. Fig. 4a and 4c illustrate the effect of $NaBF_4$ content on σ of DAM and aged PPH composite. As demonstrated above, the addition of $NaBF_4$ to sizing only slightly affected σ of DAM PPH composites. The variation, ±2.5 %, in σ was within the standard deviation of test method (Fig. 4c). The presence of $NaBF_4$ enhanced the hygrothermal durability of PPH composites, the retention of σ monotonically increased from 75 % to 86 % as the $NaBF_4$ content increased from 0 to 0.32 wt% (Fig. 4a). Correspondingly, the relative change in σ for aged PPH composites exhibited 3−18 % improvement (Fig. 4c).

Fig. 4b and 4d show the bearing of $NaBF_4$ content on the Charpy impact toughness, a_{cU}, of DAM and aged PPH composites. The incorporation of $NaBF_4$ led to reduction in a_{cU} (Fig. 4b), a 10 % decrease in a_{cU} was observed for PPC-08, however the reduction in a_{cU} vanished gradually as $NaBF_4$ content increased, PPH-32 almost fully regained the a_{cU} of PPH-00. On the other hand, the addition of $NaBF_4$ to sizing improved the retention in a_{cU} and a similar relation was also observed for the $NaBF_4$ content with the retention in a_{cU}. Specifically, the retention in a_{cU} increased from 32 % to 51 % when $NaBF_4$ content increased from 0 up to

0.32 wt% (Fig. 4b), which corresponds to a 50 % relative Charpy impact toughness improvement (Fig. 4d).

In contrast to PPH composites, PPC composites showed an insignificant effect of $NaBF_4$ on σ for both DAM and aged composites (Fig. 5a and 5c). The reason was demonstrated above. Embedding $NaBF_4$ into sizing also had no important influence on a_{cU} of DAM PPC composites (Fig. 5b and 5d). On the other hand, a great improvement in a_{cU} of aged PPC composites was found. Aged PPC composites without $NaBF_4$ only recovered 37 % of Chapry impact toughness, while the addition of 0.32 wt% $NaBF_4$ led to a 70 % retention in a_{cU} (Fig. 5b), it means that a 90% improvement could be obtained (Fig. 4d). All these further suggest that the embedded $NaBF_4$ could enhance the hygrothermal durability for both PPH and PPC based composites, the improvement in the hygrothermal durability of PPC composite is more pronounced compared to that of PPH composites.

3.3 Fractographies of broken composites

The fracture surfaces of tensile test specimens were subjected to FE-SEM investigation to deepen the understanding on the operating micromechanism of the improved hygrothermal stability. Short GF/PP composites prepared by injection moulding usually develop the skin layers dominated skin-core structure [28], where GFs are mostly oriented along the injection flow direction in the skin layers while alignment of GFs transverse to the injection flow direction is dominated in the core layers [29]. Hence, SEM images of both the skin layers and core layers of DAM and aged composites are presented in Fig. 6 and 7 for PPH and PPC composites, respectively. Fig. 6 clearly shows good fibre/matrix adhesion in the skin layers for all DAM PPH composites as manifested by the coverage of polymer matrix on the surface of pulled-out fibres. On the other hand, in the core layers of PPH-00 and PPH-08 the matrix seemed to be completely detached from the fibres, indicating poor fibre/matrix adhesion. In sharp contrast, good fibre/matrix adhesion was observed in the core layers of PPH-16 and PPH-32. This is an indication that the presence of efficient amount of $NaBF_4$ could improve

the fibre/matrix adhesion. The observed constant ultimate tensile strength for DAM PPH composites could be explained by the much lower contribution of energy absorption due to fibre/matrix debonding, crazing and void formation in the core layers with respect to the contribution of more energy consuming fibre fracture, fibre pull-out, fibre/matrix debonding caused by matrix shear, and crazing initiated at fibre ends in the skin layers [6]. As expected, hygrothermal aging led to the degradation in fibre/matrix adhesion, hence the pulled-out fibres in skin layers of aged PPH-00 and PPH-08 were nearly bare. However, it was found that aged PPH-16 exhibited less interfacial debonding at the root of the pulled-out fibres compared with aged PPH-00 and PPH-08, meanwhile the pulled-out fibre surface was partly covered with polymer matrix. Furthermore, aged PPH-32 did not show interfacial debonding and the pulled-out fibres were covered with a thin layer of polymer matrix. In other words, the failure mode changed slowly from adhesive failure to cohesive failure due to the gradual improvement in fibre/matrix adhesion strength as the $NaBF_4$ content increased. Thus, the long term performance of PPH based composites improved.

DAM PPC composites exhibited different fractography (Fig. 7), good fibre/matrix adhesion was observed for all composites either in the skin layers or in the core layers. In addition, plastic deformation of matrix polymers and micro-voids were observed, this is attributed to the enhanced stretching of PPC which has less crystallinity compared to PPH [30]. Hygrothermal aging made less detriment on PPC composites compared to PPH composites; for aged PPC-00 no debonding was determined at the root of the pulled-out fibres in the core layers, even though fibre/matrix debonding took place in the skin layers. In addition, no plastic deformation of matrix polymers, i.e. enbrittlement of matrix, was observed in the skin layers. These are consistent with the observation of the reduction in elongation at break and the constant ultimate tensile strength for aged PPC-00. The application of $NaBF_4$ gave rise to similar effect on the fibre/matrix adhesion strength as in the case of PPH composites. These

observations further confirm that the enhanced hygrothermal durability of composites with $NaBF_4$ in the interphase is related to the enhanced fibre/matrix adhesion.

3.4 Interfacial adhesion properties

To further deepen the influence of sizing formulation on the interphase adhesion behaviour, micromechanical tests of model composites were investigated by means of the single fibre pull-out test. The calculated results of interfacial adhesion strength, τ_d, frictional strength, τ_f, as well as critical energy release rate, G_{ic} for selected fibre–matrix systems are summarized in Table 2. As expected, model composites with $NaBF_4$ in the interphase showed higher interfacial adhesion strength in comparison with the reference model composites, indicating enhanced fibre/matrix adhesion strength. On the other hand, the interphase adhesion properties of model composites based on PPC were lower than those of model composites based on PPH. From the AFM topography images (Fig. 8), one can find that the fracture surfaces of pulled-out fibres were extensively covered with matrix/sizing materials. This indicates that cohesive failure occurred for both PPH and PPC based composites, which is in good agreement with SEM images on the fracture surfaces of macro-composites. The cohesive failure mechanism can account for the lower interphase adhesion properties of PPC based model composites, since PPC has lower strength compared to PPH. It might also suggest that the interphase strength of model composites with $NaBF_4$ was higher than that of reference model composites.

4. Conclusion

Short glass fibre (GF) reinforced polypropylene (PP) composites with enhanced hygrothermal durability were obtained by applying $NaBF_4$ in the sizing, in turn in the interphases of composites. The incorporation of $NaBF_4$ did not affect the surface topography, surface roughness and surface hydrophobicity of sized glass fibres. On the other hand, the surface chemical composition of differently sized GFs varied with the amount of added $NaBF_4$, monotonic increase in $NaBF_4$ and PP film former contents in the outmost surface of sized GFs

were observed with increasing $NaBF_4$ content, which gave rise to composites with enhanced fibre/matrix adhesion strength. The improvement in hygrothermal durability of composites depended on the amount of $NaBF_4$, the retention in both ultimate tensile strength, σ, and Charpy impact toughness, a_{cU}, increased monotonically with increasing $NaBF_4$ content. Specifically, linear correlation between $NaBF_4$ content and the retention in σ and a_{cU} were identified at lower $NaBF_4$ contents, while deviation from linearity was observed at 0.32 wt% $NaBF_4$. Moreover, composites based on polypropylene-polyethylene copolymers showed better hygrothermal stability in comparison with composites based on PP homopolymers. The application of $NaBF_4$ had a more pronounced improvement in the retention of the Charpy impact toughness of copolymer based composites compared to that of homopolymer based composites. Further investigation will focus on the chemistry involved for the enhanced fibre/matrix adhesion strength and the influence of $NaBF_4$ on the interphase properties, such as micro-mechanical and thermal properties. That information will deepen our knowledge about the acting mechanism of improved hygrothermal durability, which will inspire new strategies aiming to extend the application of glass fibre reinforced PP in more harsh conditions.

Acknowledgment: This work was supported by the German Research Foundation (DFG) within priority program SPP 1369 ‘‘Polymer–Solid Contacts: Interfaces and Interphases’’. We thank F. Eberth, D. Ehnert, T. Förster, Dr. S.-L. Gao, Dr. R. Häßler, J. Hiller, M. Liese, M. Oelmann, J. Rausch, H. Scheibner, B. Schulze, and Dr. F. Simon for experimental assistance.

Appendix

C 1s and N 1s high resolution spectra

The C 1s and N 1s high resolution spectra (Fig. A) were curve-fitted with four peaks and two peaks, respectively. The corresponding peak assignments are listed in Table A. The peaks of interest are C-1 and C-2, which correspond to C-C and C-N/C-O chemical states, respectively. The N-1 and N-2 are assigned to amine and protonated amine chemical states. As expected, GF-08 and GF-16 had similar C-1 at% but lower C-2 at% as reference fibre GF-00, while GF-

32 showed the highest C-1 at% and the lowest C-2 at%. It indicates that sized GFs with $NaBF_4$, especially GF-32, had higher PP film former content in sizing/air interface compared to GF-00. Additionally, it was found that the at% of N-2 increased with increasing $NaBF_4$ content, but dropped a little bit for GF-32. In the absence of $NaBF_4$, the protonation of amine groups is mainly attributed to the intramolecular and intermolecular interactions between amino groups and silanol groups as well as the interaction between amino groups and environmental carbonic acid [15, 31, 32]. The increase in N-2 at% of sized GFs with $NaBF_4$ confirms the presence of $NaBF_4$ in sized GF surfaces, since BF_4^- has high association constant and hydrophobicity, which are in favor of the formation of BF_4^-/N^+ associations [33, 34]. The small drop in N-2 at% of GF-32 could be related to its higher PP film former content in air/sizing interface as revealed by the C 1s high resolution spectra.

References

[1] Karger-Kocsis J. Preface. In: Karger-Kocsis J, ed. *Polypropylene: Structure and morphology*. Cambridge: Chapman & Hall 1999:xi-xii.
[2] Balow MJ. Global trends for polypropylene. In: Karian HG, ed. *Handbook of polyproylene and polypropylene composites, second edition, revised and expanded*. New York: Marcel Dekker, Inc. 2003.
[3] Tokaji K, Shiota H, Ogawa T, Yumitori S. Tensile and fatigue properties of long glass fibre-reinforced polypropylene immersed in hot water. J Mater Sci 1998;33(19):4739-45.
[4] Flowers B. Automotive applications for polypropylene and polypropylene composites. In: Karian HG, ed. *Handbook of polypropylene and polypropylene composites, second edition, revised and expanded*. New York: Marcel Dekker, Inc. 2003.
[5] Srivastava VK, Hogg PJ. Moisture effects on the toughness, mode-I and mode-II of particles filled quasi-isotropic glass–fibre reinforced polyester resin composites. J Mater Sci 1998;33(5):1129-36.
[6] Mohd Ishak ZA, Ishiaku US, Karger-Kocsis J. Microstructure-related fracture behaviour of injection moulded short fibre reinforced polyarylamide in dry and wet states. J Mater Sci 1998;33(13):3377-89.
[7] Koenig JL, Emadipour H. Mechanical characterization of the interfacial strength of glass-reinforced composites. Polym Compos 1985;6:142-50.
[8] Roy R, Sarkar BK, Bose NR. Effects of moisture on the mechanical properties of glass fibre reinforced vinylester resin composites. Bull Mater Sci 2001;24(1):87-94.
[9] Davies P, Pomies F, Carlsson LA. Influence of water absorption on transverse tensile properties and shear fracture toughness of glass/polypropylene. J Compos Mater 1996;30(9):1004-19.
[10] Jancar J. Hydrolytic stability of PC/GF composites with engineered interphase of varying elastic modulus. Compos Sci Technol 2006;66(16):3144-52.

[11] Thwe MM, Liao K. Effects of environmental aging on the mechanical properties of bamboo-glass fiber reinforced polymer matrix hybrid composites. Compos A: Appl Sci Manuf 2002;33(1):43-52.
[12] Doan TTL, Brodowsky H, Mäder E. Jute fibre/polypropylene composites II. Thermal, hydrothermal and dynamic mechanical behaviour. Compos Sci Technol 2007;67(13):2707-14.
[13] Kim JK, Mai YW. High strength, high fracture toughness fibre composites with interface control - A review. Compos Sci Technol 1991;41(4):333-78.
[14] Mäder E, Moos E, Karger-Kocsis J. Role of film formers in glass fibre reinforced polypropylene - new insights and relation to mechanical properties. Compos A: Appl Sci Manuf 2001;32(5):631-9.
[15] Zhuang RC, Burghardt T, Mäder E. Study on interfacial adhesion strength of single glass fibre/polypropylene model composites by altering the nature of the surface of sized glass fibres. Compos Sci Technol 2010;70(10):1523-9.
[16] Trzpit M, Soulard M, Patarin J, Desbiens N, Cailliez F, Boutin A, et al. The effect of local defects on water adsorption in silicalite-1 zeolite: A joint experimental and molecular simulation study. Langmuir 2007;23(20):10131-9.
[17] Ishak ZAM, Yow BN, Ng BL, Khalil HPSA, Rozman HD. Hygrothermal aging and tensile behavior of injection-molded rice husk-filled polypropylene composites. J Appl Polym Sci 2001;81(3):742-53.
[18] Okabe A, Fukushima T, Ariga K, Niki M, Aida T. Tetrafluoroborate salts as site-selective promoters for sol-gel synthesis of mesoporous silica. J Am Chem Soc 2004;126(29):9013-6.
[19] Okabe A, Niki M, Fukushima T, Aida T. A simple route to bimodal mesoporous silica via tetrafluoroborate ion-mediated hydrophobic transformation of template micellar surface. J Mater Chem 2005;15(13):1329-31.
[20] Huang YX, Schäfer G, Borrmann H, Zhao JT, Kniep R. $(C_2H_{10}N_2)[BPO_4F_2]$ - Structural relations between $[BPO_4F_2]_2^-$ and $[Si_2O_6]_4^-$. Z Anorg Allg Chem 2003;629(1):3-5.
[21] Freire MG, Neves CMSS, Marrucho IM, Coutinho JAP, Fernandes AM. Hydrolysis of tetrafluoroborate and hexafluorophosphate counter ions in imidazolium-based ionic liquids. J Phys Chem A 2009;114(11):3744-9.
[22] Mäder E, Gao SL, Plonka R, Wang J. Investigation on adhesion, interphases, and failure behaviour of cyclic butylene terephthalate (CBT®)/glass fiber composites. Compos Sci Technol 2007;67(15-16):3140-50.
[23] Zhuang RC, Burghardt T, Plonka R, Liu JW, Mäder E. Affecting glass fibre surfaces and composite properties by two stage sizing application. eXPRESS Polym Lett 2010;4(12):798-808.
[24] Thomason JL, Dwight DW. The use of XPS for characterisation of glass fibre coatings. Compos A: Appl Sci Manuf 1999;30(12):1401-13.
[25] Tai CM, Li RKY, Ng CN. Impact behaviour of polypropylene/polyethylene blends. Polym Testing 2000;19(2):143-54.
[26] Yow BN, Ishiaku US, Ishak ZAM, Karger-Kocsis J. Kinetics of water absorption and hygrothermal aging rubber toughened poly(butylene terephthalate) with and without short glass fiber reinforcement. J Appl Polym Sci 2004;92(1):506-16.
[27] Thwe MM, Liao K. Durability of bamboo-glass fiber reinforced polymer matrix hybrid composites. Compos Sci Technol 2003;63(3-4):375-87.
[28] Katti SS, Schultz M. The microstructure of injection-molded semicrystalline polymers: A review. Polym Eng Sci 1982;22(16):1001-17.
[29] Hegler RP, Mennig G. Phase separation effects in processing of glass-bead- and glass-fiber-filled thermoplastics by injection molding. Polym Eng Sci 1985;25(7):395-405.
[30] Dasari A, Rohrmann J, Misra RDK. Surface microstructural modification and fracture behavior of tensile deformed polypropylene with different percentage crystallinity. Mater Sci Eng A 2003;360(1-2):237-48.

[31] Bascom WD. Structure of silane adhesion promoter films on glass and metal surfaces. Macromolecules 1972;5(6):792-8.
[32] Naviroj S, Culler SR, Koenig JL, Ishida H. Structure and adsorption characteristics of silane coupling agents on silica and E-glass fiber; dependence on pH. J Colloid Interf Sci 1984;97(2):308-17.
[33] Zhou Y. Recent advances in ionic liquids for synthesis of inorganic nanomaterials. Curr Nanosci 2005;1(1):35-48.
[34] Yu B, Zhou F, Liu G, Liang Y, Huck WTS, Liu W. The electrolyte switchable solubility of multi-walled carbon nanotube/ionic liquid (MWCNT/IL) hybrids. Chem Commun 2006;(22):2356-8.

Figure Captions

Figure 1. Typical 3D AFM height images of differently sized GFs. From left to right: GF-00, GF-08, GF-16, and GF-32. Scan size: 3×3 μm, Z data scale: 250 nm.

Figure 2. XPS survey spectra of GF-00 (top) and GF-08 (bottom)

Figure 3. Typical stress-strain curves for composites before and after hygrothermal aging. The inset shows the color development for composites after hygrothermal aging.

Figure 4. Impact of $NaBF_4$ content on the ultimate tensile strength (a, c) and Charpy impact toughness (b, d) of PPH composites before and after aging: a) tensile strength of DAM and aged composites and the retention of tensile strength after hygrothermal aging, b) Charpy impact toughness of DAM and aged composites and the retention of Charpy impact toughness after hygrothermal aging, c) relative tensile strength change for PPH composites, d) relative Charpy impact toughness change for PPH composites.

Figure 5. Impact of $NaBF_4$ content on the ultimate tensile strength (a, c) and Charpy impact toughness (b, d) of PPC composites before and after aging: a) tensile strength of DAM and aged composites and the retention of tensile strength after hygrothermal aging, b) Charpy impact toughness of DAM and aged composites and the retention of Charpy impact toughness after hygrothermal aging, c) relative tensile strength change for PPH composites, d) relative Charpy impact toughness change for PPH composites.

Figure 6. FE-SEM images of the fracture surfaces of DAM and aged PPH composites

Figure 7. FE-SEM images of the fracture surfaces of DAM and aged PPC composites

Figure 8. AFM topography images (scan size: 3× 3μm) of GF-00 after pull-out from PPH (left, Z data scale: 900 nm) and PPC (right, Z data scale: 1200 nm).

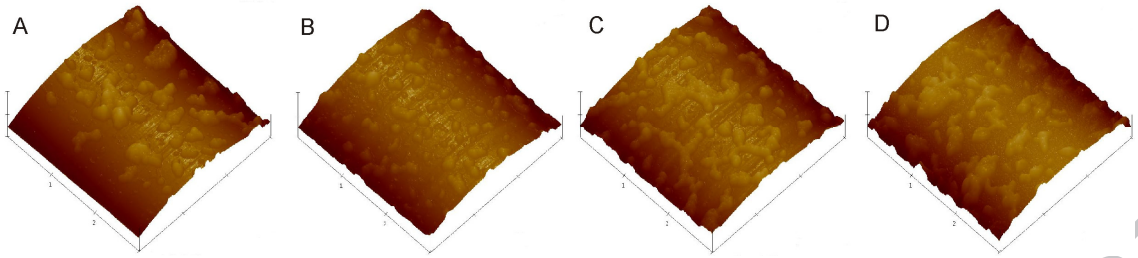

Figure 1.

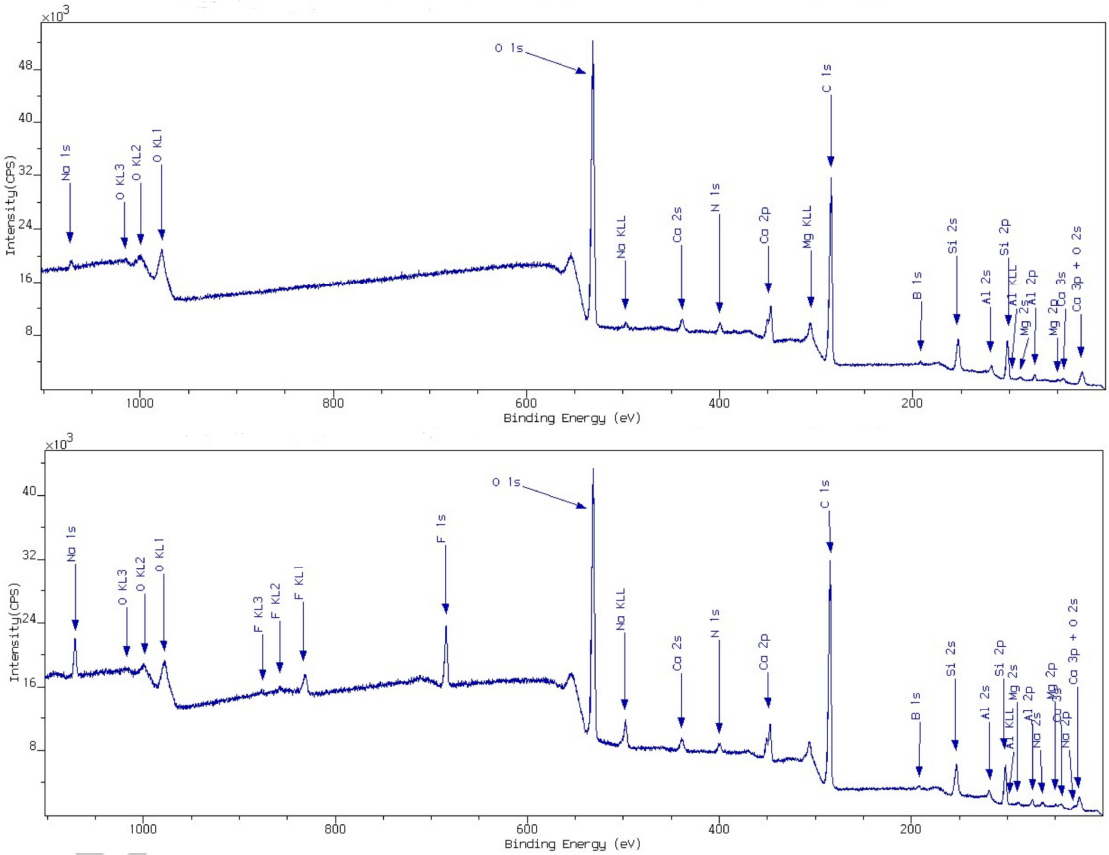

Figure 2.

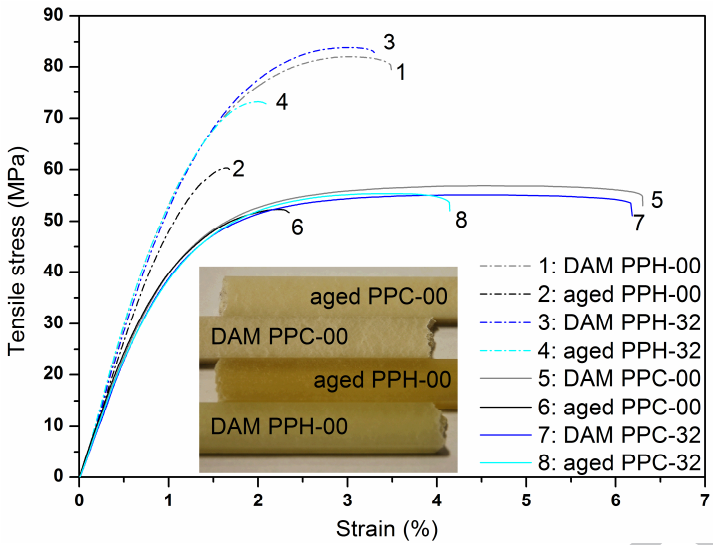

Figure 3.

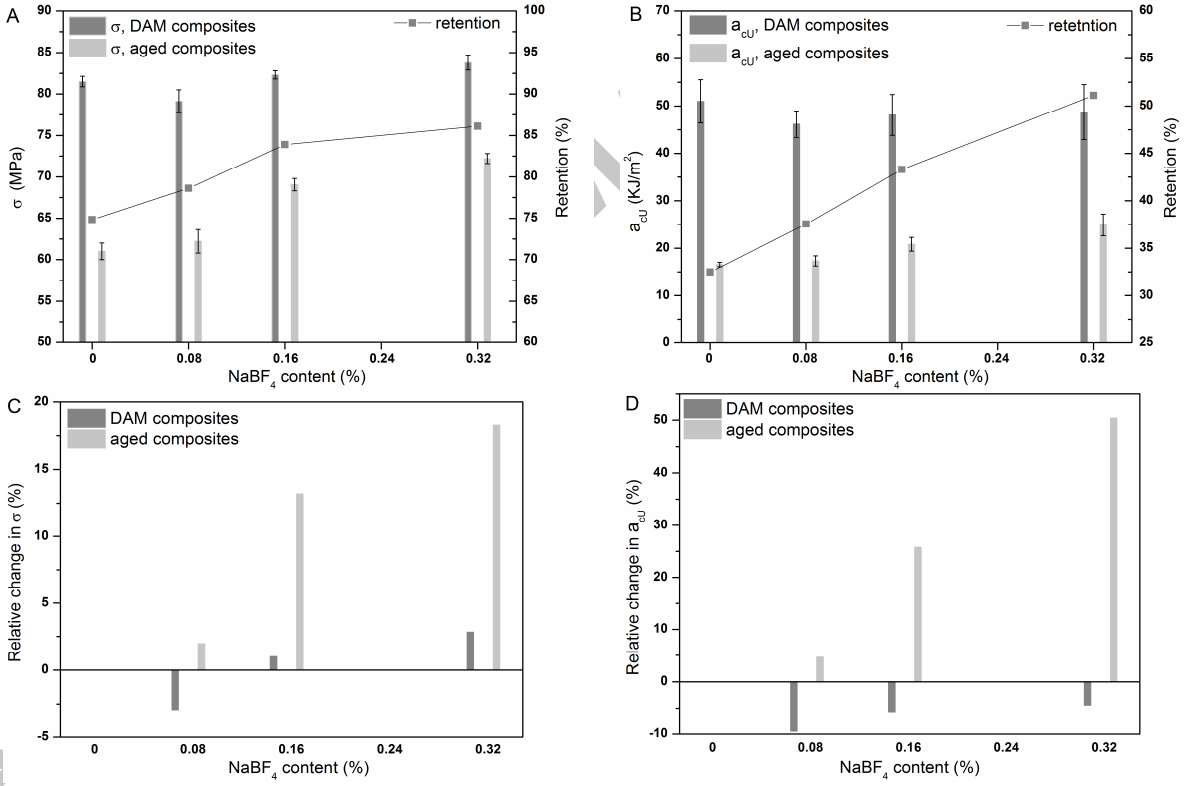

Figure 4.

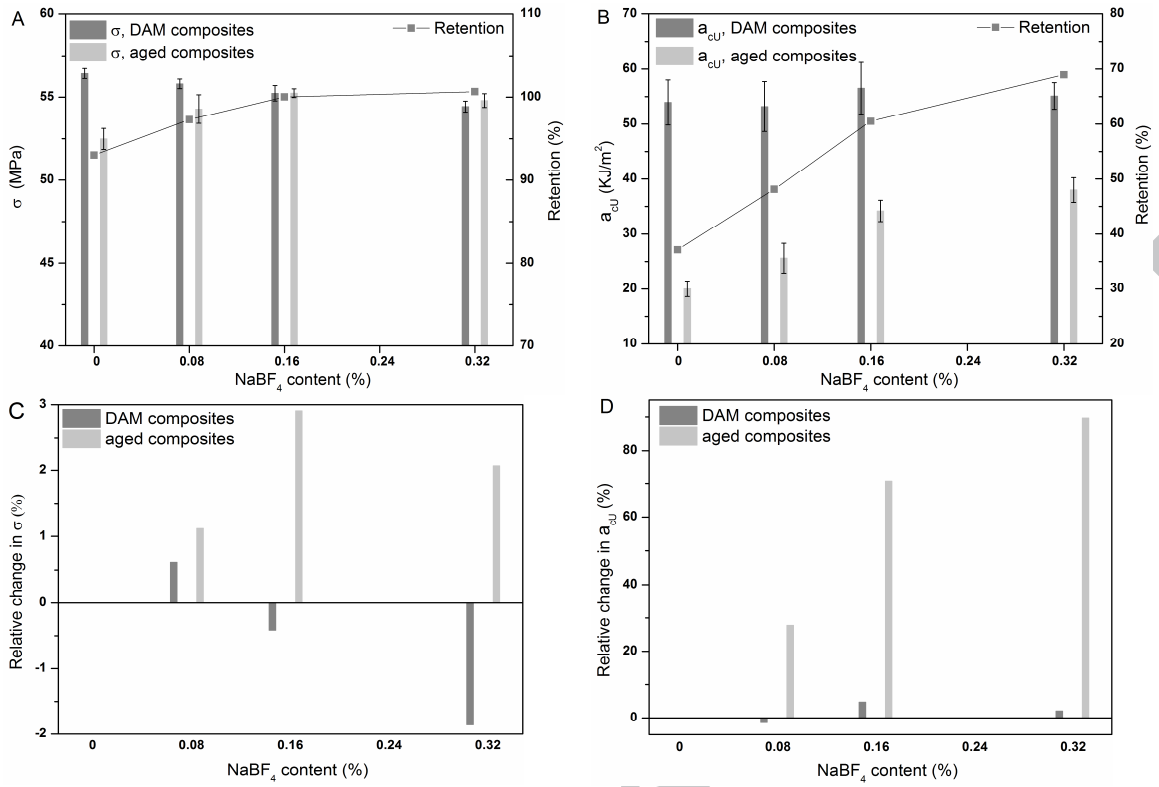

Figure 5.

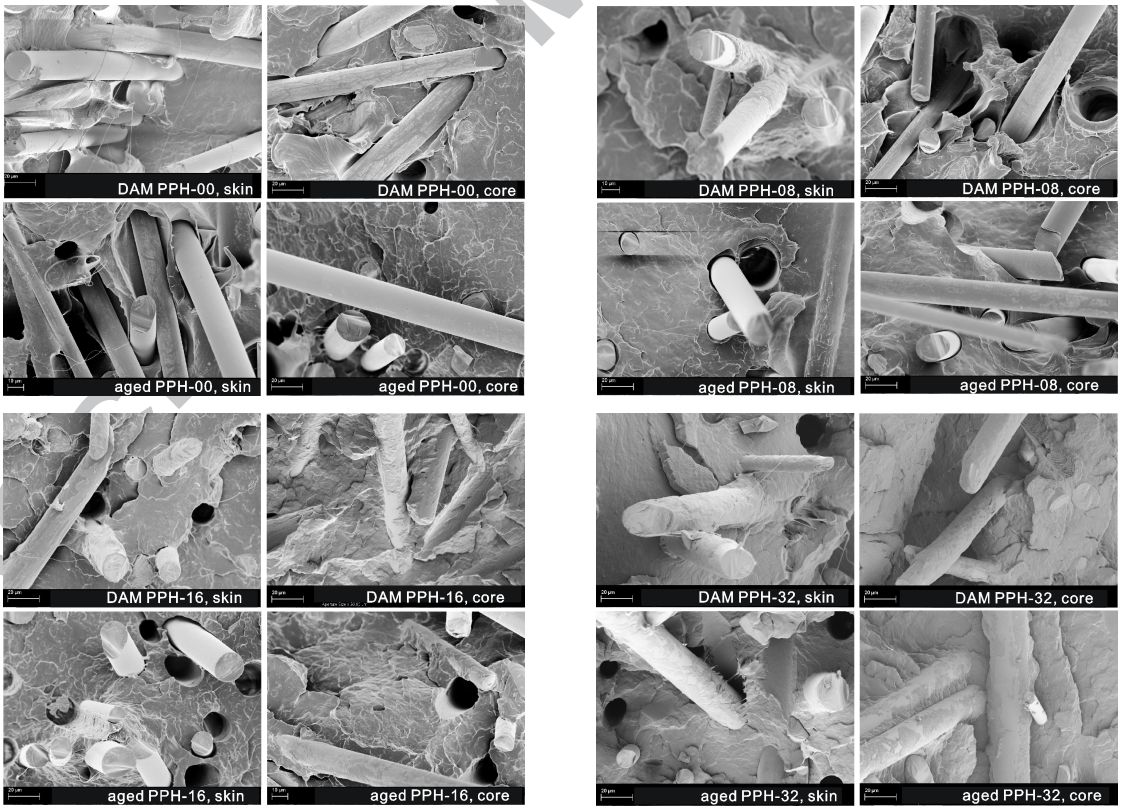

Figure 6.

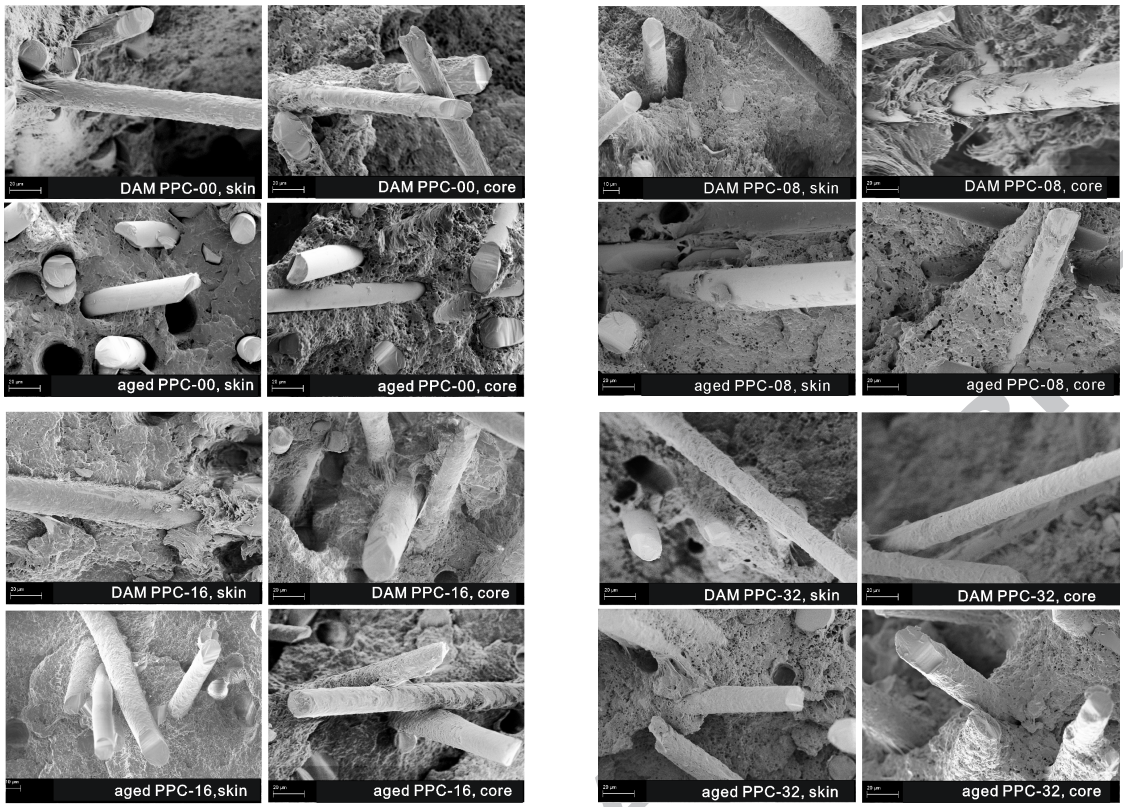

Figure 7.

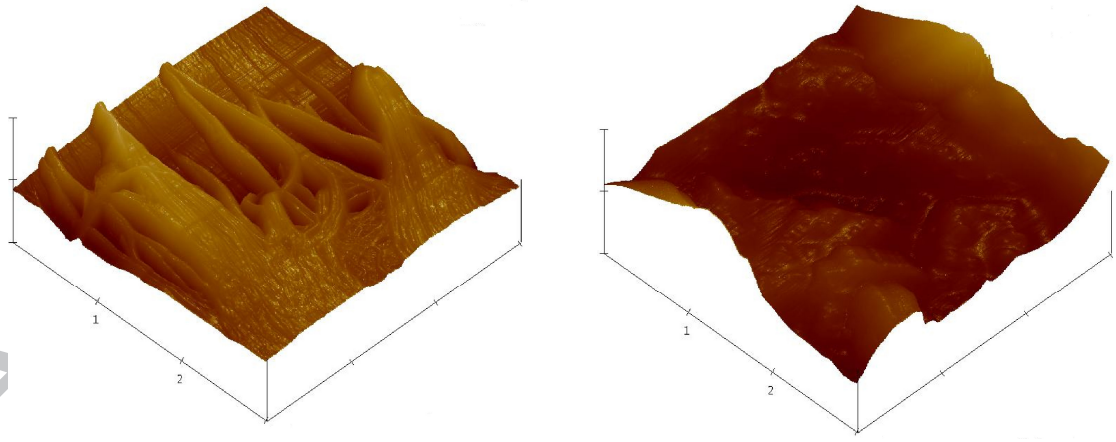

Figure 8.

Table 1. Surface property comparison for differently sized glass fibres in terms of LOI, surface roughness, dynamical contact angles, and normalized average surface compositions (in at%)

GF	LOI (wt%)	Roughness (nm)		Contact angle (deg)		Normalized average surface compositions (at%)						
		R_q	R_{max}	θ_a	θ_r	Na/Ca	O/Ca	N/Ca	C/Ca	B/Ca	Si/Ca	F/Ca
GF-00	0.30	11.6±5.5	110.7±44.2	84.7±1.5	61.0±2.9	0.3	18.1	1.1	35.9	1.5	6.5	0
GF-08	0.34	9.2±3.0	81.3±17.4	84.0±3.3	60.9±2.3	1.0	15.8	0.9	40.7	1.1	6.1	2.4
GF-16	0.34	10.1±3.5	93.1±26.3	83.0±2.3	62.6±4.3	2.0	13.4	1.0	40.9	1.6	5.0	4.6
GF-32	0.57	12.9±5.1	121.2±38.4	84.0±4.5	52.6±3.8	2.0	12.2	0.7	55.2	1.3	4.2	5.1

Table 2. Summary of interphase adhesion properties in terms of interfacial adhesion strength, τ_d, frictional strength, τ_f, and critical interfacial energy release rate, G_{ic}

GF	Matrix	τ_d (MPa)	τ_f (MPa)	G_{ic} (J/m^2)
GF-00	PPH	7.52	4.43	13.76
GF-08	PPH	8.90	6.49	21.52
GF-32	PPH	8.47	5.28	13.77
GF-00	PPC	5.83	2.68	10.51
GF-08	PPC	6.26	3.29	11.68

Figure Caption for Appendix

Figure A. Typical C 1s (left) and N 1s (right) high resolution spectra and corresponding curve fitting and peak assignment

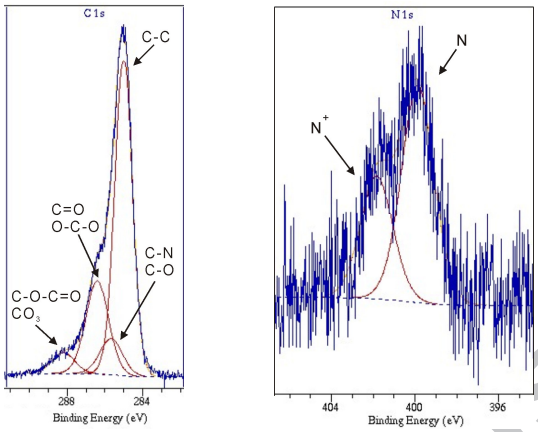

Figure A.

Table A. Average C and N surface compositions (in at%) of differently sized glass fibres

GF	C surface composition				N surface composition	
	C-1	C-2	C-3	C-4	N-1	N-2
GF-00	67.6	7.8	20.1	4.5	63.8	36.2
GF-08	70.4	5.3	21.3	3.0	54.0	46.0
GF-16	70.9	6.3	18.9	3.9	48.0	52.0
GF-32	82.4	3.2	12.5	2.0	54.9	45.1
Binding energy (eV)	285.0	286.4-286.5	287.4-287.5	288.7-289.0	399.9	401.9
Chemical state	C-C	C-N/C-O	C=O/O-C-O	C-O-(C=O)/CO_3	N	N^+

Researchhighlights CSTE 5001

- $NaBF_4$ as glass fibre/PP composite hygrothermal durability enhancer
- Glass fibre surface morphology remains unchanged
- Surface chemical compositions revealed as expected
- Copolymer based composites show higher hygrothermal stability
- Hygrothermal durability monotonically increases with increasing $NaBF_4$ content